processes

Article

A Simulation Study of an Electro-Hydraulic Load-Sensitive Variable Pressure Margin Diverter Synchronous Drive System with Time-Varying Load Resistance

Wei Du, Yu Luo *, Yanlei Luo and Hongyun Mu

School of Mechanical Engineering, Guizhou University, Guiyang 550025, China; 18738749123@163.com (W.D.); ylluo@gzu.edu.cn (Y.L.); muhongyungzdx@163.com (H.M.)
* Correspondence: yluo6@gzu.edu.cn; Tel.: +86-138-851-89830

Abstract: This study aims to address the problem of poor synchronous accuracy when facing a time-varying load in conventional load-sensitive synchronous drive systems. The new electro-hydraulic load-sensitive (EHLS) diverter synchronous drive system was proposed by combining the diverter valve and the EHLS synchronous drive system. The variable pressure margin compensation control was proposed to further improve the system's synchronous control performance. Based on the system control strategy and component mathematical model, the simulation models of the EHLS, EHLS synchronous, and EHLS diverter synchronous drive systems were established using AMESim, respectively, and the synchronous control performance of the systems was obtained. The simulation results show that the EHLS drive system realized the primary functions of the load-sensitive system and could realize the variable load-sensitive pressure margin control. The EHLS synchronous drive system had poor synchronous control accuracy, but variable pressure compensation valve pressure margin control could be realized. The EHLS diverter synchronous drive system effectively improved the system's synchronous control performance and diverter synchronous accuracy by variable pressure margin compensation control. The diverter system diverter error was reduced by 40.8%, and the diverter system after the compensation diverter error was reduced by 52.6% when the multi-way valves were fully opening. The system provides the solution for high-performance hydraulic synchronous drives under severe operating conditions.

Keywords: EHLS; variable pressure margin compensation control; diverter valve; synchronous drive; simulation

Citation: Du, W.; Luo, Y.; Luo, Y.; Mu, H. A Simulation Study of an Electro-Hydraulic Load-Sensitive Variable Pressure Margin Diverter Synchronous Drive System with Time-Varying Load Resistance. *Processes* **2024**, *12*, 170. https://doi.org/10.3390/pr12010170

Academic Editors: Xavier Escaler, Zhengwei Wang, Xingxing Huang, Cristian Rodriguez and Quanwei Liang

Received: 16 September 2023
Revised: 7 October 2023
Accepted: 11 October 2023
Published: 11 January 2024

1. Introduction

In recent years, the international community has attached increasing importance to developing the green economy, realizing "carbon neutrality" has become a significant development goal in the future [1,2]. To achieve zero emissions, off-road mobile machines and industrial hydraulics are also embracing the era of electrification, i.e., variable speed hydraulics will be the mainstay of future development.

The EHLS systems are typical applications of variable speed hydraulics technology, where the speed of the motor is controlled to match the pressure and flow of the system. Because the system has the advantages of fast response speed, strong self-adaptation, and smooth operation [3], it is widely used in electromechanical equipment. The development of electromechanical equipment technology has led to large-scale and heavy-duty developments [4,5]. This also increases the need for hydraulic synchronous drive technology for heavy loads. Hydraulic synchronous technology is used in various engineering applications [6–8]. High-precision, high-reliability, and high-efficiency hydraulic synchronous drives have been an important research topic and problem in hydraulics [9]. Hydraulic synchronous drive control consists of two primary forms of control: hydraulic synchronous closed-loop control and hydraulic synchronous open-loop control [10].

For hydraulic synchronous closed-loop control, scholars have carried out much research [11]. Ma [12] proposed the improved automatic anti-interference controller-improved particle swarm optimized position synchronous control method to solve the problem of insufficient platform synchronous control accuracy of the multi-hydraulic cylinder group platform of an anchor digging support robot. The results show that the method has better position tracking performance and shorter adjustment time, its stepping signal synchronous error was controlled within 5.0 mm, and the adjustment time was less than 2.55 s. Ding [13] proposed the robust output feedback position controller to solve the problem of the poor robustness of the conventional PID controller of the hydraulic support. The results show that the tracking accuracy of this controller was 47.2% and 30.6% higher than the conventional controller, respectively. Guo [14] proposed the synchronous controller based on improved sliding mode control for the hydraulic strut system. The results show that the controller could effectively reduce the synchronous error between the positions of two hydraulic struts and had better control performance than the PI and fuzzy PID controllers. Zhu [15] proposed the control method with dual closed-loop composite robustness to solve the performance deficiencies of the dual-pump dual-valve-controlled motor, such as poor output speed stability, low controllability, and difficulty in synchronous output management under external disturbances. The results show that the control method had high accuracy and robustness. Jing [16] proposed a load disturbance decoupling control method and developed a two-cylinder synchronous control system to meet the high precision control requirements of the system. The results show that the system's robustness was improved. Therefore, most controllers were combined with optimization algorithms for hydraulic synchronous closed-loop control. Although it effectively improved the synchronous control performance of the system, the system was more complex and costly [17].

Hydraulic synchronous open-loop control is mainly based on the load-sensitive system. Hu [18] proposed the new pile-pressing hydraulic control system based on the design of the load-sensitive pump aimed at the problem of unsynchronous movement of pile-pressing cylinders during the pile pressing of a hydraulic static pile driver. The results show that the system had good synchronous control performance. Yang [19] used load-sensitive control for the two-cylinder synchronous drive to demand the high-efficiency, adjustable-speed, and high-precision synchronous drive system. The results reveal the primary factors and laws that affect the synchronous accuracy of the system. Wang [20] used the load-sensitive principle for the open-loop synchronous loop of the stent from the point of view of energy saving and high efficiency. The results show that this synchronous system's displacement and velocity synchronous error were small. Therefore, the hydraulic synchronous open-loop control was mainly applied to the occasions where synchronous accuracy was not required. Although the hydraulic synchronous open-loop control is relative to the hydraulic synchronous closed-loop control, synchronous control accuracy is poor. The research of a new high-precision hydraulic synchronous open-loop control system is also significant, considering the cost.

Based on the above analysis, this study combined the EHLS synchronous drive system with the diverter valve diverter synchronous technology to construct a new EHLS diverter synchronous drive system. The contributions of this research are as follows:

(1) The EHLS drive system was constructed, and variable load-sensitive pressure margin control was realized;
(2) The diverter valve diverter synchronous technology was used in the EHLS synchronous drive system to construct the EHLS diverter synchronous drive system. It effectively improved the diverter synchronous accuracy of the system. However, it reduced the synchronous control performance of the system;
(3) The solenoid pressure compensation valve replaced the conventional pressure compensation valve. The variable pressure compensation valve pressure margin control was realized;

(4) The system synchronous control performance was ensured, and the system diverter synchronous accuracy was improved by variable pressure margin control.

This paper is structured as follows. Section 2 is the analysis of the system's working principle. Section 3 is the analysis of the system control strategy. Section 4 is the analysis of the components' mathematical model. Section 5 is system modeling and simulation. Section 6 is the discussion. Furthermore, Section 7 is the conclusion.

2. Analysis of the System's Working Principle

This part analyzes the working principle and drawbacks of the conventional EHLS synchronous drive system. The new EHLS diverter synchronous drive system is proposed based on the conventional system, and the system's working principle is analyzed.

2.1. Analysis of the Working Principle of the Conventional System

A conventional and typical EHLS synchronous drive system [21–23] is shown in Figure 1. The permanent magnet synchronous motor (PMSM), 1, drives a quantitative pump, 2, to generate high-pressure oil. The high-pressure oil enters the pressure compensation valves, 6 and 7, through the multi-way valves, 4 and 5, respectively, and the oil from the pressure compensation valves, 6 and 7, enters the synchronous actuator, 8, which causes the synchronous actuator, 8, to perform synchronous actions.

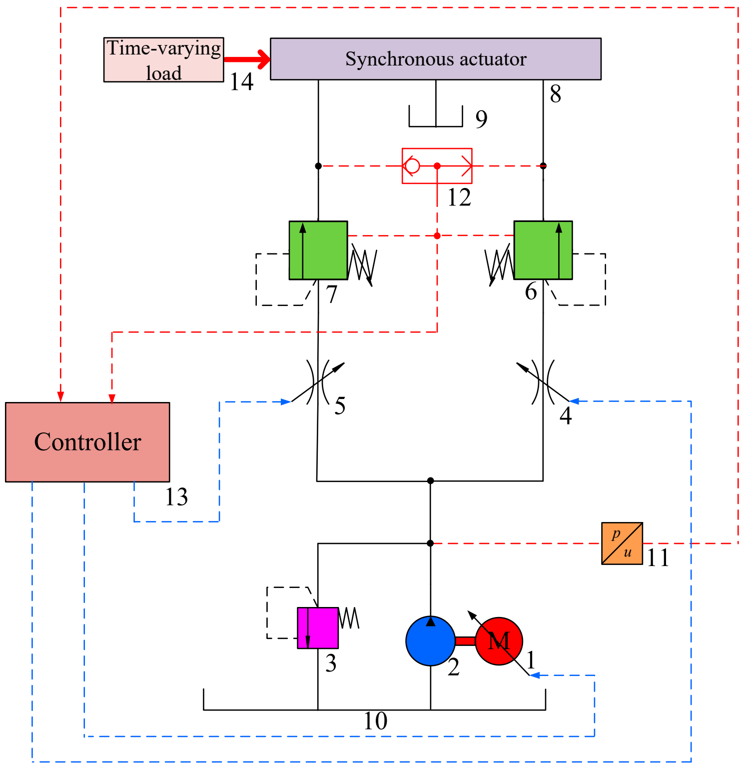

Figure 1. Schematic diagram of the conventional typical EHLS synchronous drive system. 1. PMSM. 2. Quantitative pump. 3. Safety valve. 4, 5. Multi-way valve. 6, 7. Conventional pressure compensation valve. 8. Synchronous actuator. 9, 10. Tank. 11. Pressure sensor. 12. Shuttle valve. 13. Controller. 14. Time-varying load.

The multi-way valve openings are the same for load-sensitive synchronous drive systems during operation. The pressure compensation valves, 6 and 7, eliminate flow rate errors caused by static load variation. However, the load is mostly time-varying when the synchronous actuator, 8, performs synchronous actions. The pressure compensation valves are slow to respond and do not eliminate time-varying loads. Furthermore, the system uses pressure feedback closed-loop control to control the system pressure and flow rate.

When the load changes, it will inevitably cause the system pressure and flow rate to change, reducing the system's synchronous accuracy. When the actuator requires high synchronous accuracy, it is difficult for the system to meet the requirements. Therefore, it is necessary to improve the system's synchronous accuracy.

2.2. Analysis of the Working Principle of the New System

The diverter valve diverter synchronous technology is introduced into the typical EHLS synchronous drive system to improve the synchronous accuracy of the conventional drive system when facing a time-varying load. The new EHLS diverter synchronous drive system is constructed, as shown in Figure 2. The system is compared with the conventional system. The diverter valve, 18, is added between the quantitative pump, 2, and the multi-way valves, 4 and 5. It can improve the system diverter synchronous accuracy. A solenoid pressure compensation valve replaces the conventional pressure compensation valve. It can improve the response speed of the pressure compensation valve and reduce the impact of time-varying load on the synchronous system. When the system load is a time-varying load, the system can effectively improve the synchronous accuracy of the system through the diverter effect of the diverter valve and the compensation effect of the solenoid pressure compensation valve.

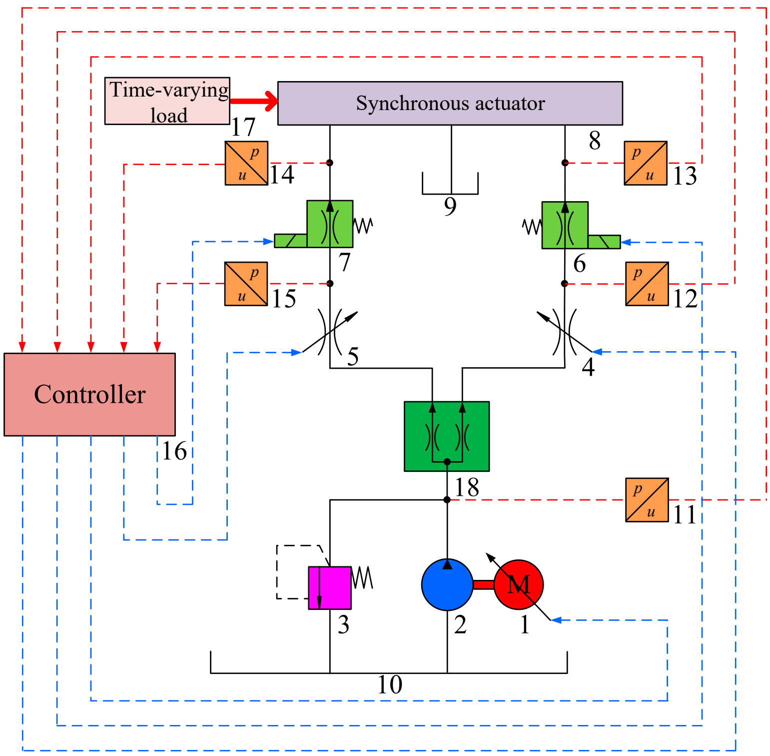

Figure 2. Schematic diagram of the new EHLS diverter synchronous drive system. 1. PMSM. 2. Quantitative pump. 3. Safety valve. 4, 5. Multi-way valve. 6, 7. Solenoid pressure compensation valve. 8. Synchronous actuator. 9, 10. Tank. 11, 12, 13, 14, 15. Pressure sensor. 16. Controller. 17. Time-varying load. 18. Diverter valve.

3. Analysis of System Control Strategy

This section analyzes the variable speed control, the variable load-sensitive pressure margin control, and the variable pressure compensation valve pressure margin control.

3.1. Variable Speed Control

The system utilizes a combination of the quantitative pump and the PMSM. The PMSM speed is adjusted to control the quantitative pump outlet pressure and flow rate using pressure feedback closed-loop control.

The quantitative pump outlet target pressure can be described as [24]:

$$p_{p'} = p_{Max} + \Delta p_{Ls} \tag{1}$$

where $p_{p'}$ is the target pressure of the quantitative pump, Pa; p_{Max} is the maximum load pressure, Pa; and Δp_{Ls} is the load-sensitive preset pressure margin, Pa.

The quantitative pump outlet pressure error can be described as [24]:

$$e_p = p_{p'} - p_p \tag{2}$$

where e_p is the quantitative pump outlet pressure error, Pa, and p_p is the actual pressure of the quantitative pump outlet, Pa.

The PMSM target torque can be obtained using e_p as the PID controller inlet, and then the PMSM target torque can be described as [24]:

$$T(e_p) = k_p e_p + k_i \int e_p dt + k_d \dot{e}_p \tag{3}$$

where $T(e_p)$ is the PMSM target torque, N·m; k_p is the scaling factor; k_i is the integration coefficient; and k_d is the differentiation coefficient.

The PMSM target speed can be described as [24]:

$$n_{ref} = f(e_p) = \frac{9550P}{T(e_p)} \tag{4}$$

where n_{ref} is the PMSM target speed, rev/min, and P is the PMSM rated power, kW.

It can be seen in Equations (1)–(4) that when p_{Max} changes dynamically to maintain Δp_{Ls}, the PMSM target speed will also change to dynamically regulate the quantitative pump's outlet pressure and flow rate to bring the system to a new equilibrium state.

3.2. Variable Load-Sensitive Pressure Margin Control

Based on the analysis in Section 3.1, it can be seen that when Δp_{Ls} is changed, the system can maintain the new Δp_{Ls} through the pressure feedback closed-loop control. Therefore, the system can realize variable Δp_{Ls} control.

For the EHLS synchronous drive system, synchronous performance can be reflected by the flow rate of each branch.

The flow rate through the multi-way valve, 1, can be described as:

$$Q_1 = C_d w x_1 \sqrt{\frac{2(\Delta p_{Ls} - \Delta p_d)}{\rho}} = C_d w x_1 \sqrt{\frac{2(\Delta p_1)}{\rho}} \tag{5}$$

where Q_1 is the flow rate through the multi-way valve, 1, m^3/s; C_d is the flow coefficient; w is the area gradient, m; x_1 is the spool displacement of the multi-way valve, 1, m; Δp_d is the preset pressure margin of the pressure compensation valve, Pa; ρ is the oil density, kg/m^3; and Δp_1 is the pressure difference before and after the multi-way valve, 1, Pa.

The flow rate through the multi-way valve, 2, can be described as:

$$Q_2 = C_d w x_2 \sqrt{\frac{2(\Delta p_{Ls} - \Delta p_d)}{\rho}} = C_d w x_2 \sqrt{\frac{2(\Delta p_2)}{\rho}} \tag{6}$$

where Q_2 is the flow rate through the multi-way valve, 2, m^3/s; x_2 is the spool displacement of the multi-way valve, 2, m; and Δp_2 is the pressure difference before and after the multi-way valve, 2, Pa.

Ib Equations (5) and (6), Q_1 and Q_2 vary when Δp_{Ls} varies. Therefore, the variable Δp_{Ls} control can regulate the system flow rate.

Normally, the system multi-way valve openings are equal, i.e., $x_1 = x_2$. Therefore, theoretically, $Q_1 = Q_2$, i.e., the flow rate of each branch is equal. However, when time-varying loads exist in each system branch, it is difficult for the system to reach equilibrium quickly, resulting in the actual $\Delta p_1 \neq \Delta p_2$ in each branch of the system, which results in $Q_1 \neq Q_2$, i.e., the flow rate in each branch is not equal, causing the system diverter error.

For the EHLS diverter synchronous drive system, the diverter valve is added to the circuit, resulting in a system pressure loss.

The flow rate through the multi-way valve, 1, can be described as:

$$Q_{11} = C_d w x_1 \sqrt{\frac{2(\Delta p_{Ls} - \Delta p_{s1} - \Delta p_d)}{\rho}} = C_d w x_1 \sqrt{\frac{2(\Delta p_{11})}{\rho}} \tag{7}$$

where Q_{11} is the flow rate through the multi-way valve, 1, m^3/s; Δp_{s1} is the branch 1 diverter valve pressure drop, Pa; and Δp_{11} is the pressure difference before and after the multi-way valve, 1, Pa.

The flow rate through the multi-way valve, 2, can be described as:

$$Q_{22} = C_d w x_2 \sqrt{\frac{2(\Delta p_{Ls} - \Delta p_{s2} - \Delta p_d)}{\rho}} = C_d w x_2 \sqrt{\frac{2(\Delta p_{22})}{\rho}} \tag{8}$$

where Q_{22} is the flow rate through the multi-way valve, 2, m^3/s; Δp_{s2} is the branch 2 diverter valve pressure drop, Pa; and Δp_{22} is the pressure difference before and after the multi-way valve, 2, Pa.

It can be seen in Equations (7) and (8) that since the opening of the multi-way valve is equal, i.e., $x_1 = x_2$. It must satisfy $\Delta p_{11} = \Delta p_{22}$ to realize $Q_{11} = Q_{22}$. When there is a time-varying load in each branch of the system due to the diverter effect of the diverter valve, Δp_{s1} and Δp_{s2} are compensated for the system so that $\Delta p_{11} = \Delta p_{22}$, realizing $Q_{11} = Q_{22}$. Thus, the system diverter synchronous accuracy is improved.

When the opening of the multi-way valve increases, the system flow rate increases, while the throttling effect of the diverter valve is strengthened, resulting in an increase in Δp_{s1} and Δp_{s2}, which reduces Q_{11} and Q_{22}. It is necessary to satisfy $Q_1 = Q_2 = Q_{11} = Q_{22}$ to ensure the synchronous control performance of the system, as is shown in Equations (5)–(8), i.e., it is necessary to satisfy $\Delta p_1 = \Delta p_2 = \Delta p_{11} = \Delta p_{22}$. Therefore, Δp_{Ls} and Δp_d must be changed so that the system realizes $\Delta p_1 = \Delta p_2 = \Delta p_{11} = \Delta p_{22}$, i.e., the system must undergo variable pressure margin control.

3.3. Variable Pressure Compensation Valve Pressure Margin Control

The solenoid pressure compensation valve replaces the conventional pressure compensation valve to realize the variable pressure compensation valve pressure margin control.

The actual differential pressure of the solenoid pressure compensation valve can be described as [24]:

$$e_{pd} = p_n - p_{Max} \tag{9}$$

where e_{pd} is the actual differential pressure of the solenoid pressure compensation valve, Pa, and p_n is the pressure before the solenoid pressure compensation valve, Pa.

The pressure compensation valve preset differential pressure error can be described as [24]:

$$e_{pdm} = \Delta p_d - e_{pd} \tag{10}$$

where e_{pdm} is the preset differential pressure error of the solenoid pressure compensation valve, Pa.

The control current of the solenoid pressure compensation valve can be described as [24]:

$$i_c = k_p e_{pdm} + k_i \int e_{pdm} dt + k_d \dot{e}_{pdm} \tag{11}$$

where i_c is the control current of the solenoid pressure compensation valve, A.

It can be seen in Equations (9)–(11) that when p_{Max} is dynamically changed, the solenoid pressure compensation valve control current will also be changed to maintain Δp_d so that the system reaches a new equilibrium state. When Δp_d is changed, the system can maintain the new Δp_d by pressure feedback closed-loop control. Therefore, the system can realize variable Δp_d control.

Based on the analysis in Sections 3.1–3.3, a block diagram of the system control strategy can be obtained, as shown in Figure 3. Through the pressure feedback closed-loop control, the system can realize variable load-sensitive and variable pressure compensation valve pressure margin control to compensate for the pressure loss caused by the diverter valve. Under the premise of ensuring the synchronous control performance of the system, the diverter of synchronous accuracy of the system is improved.

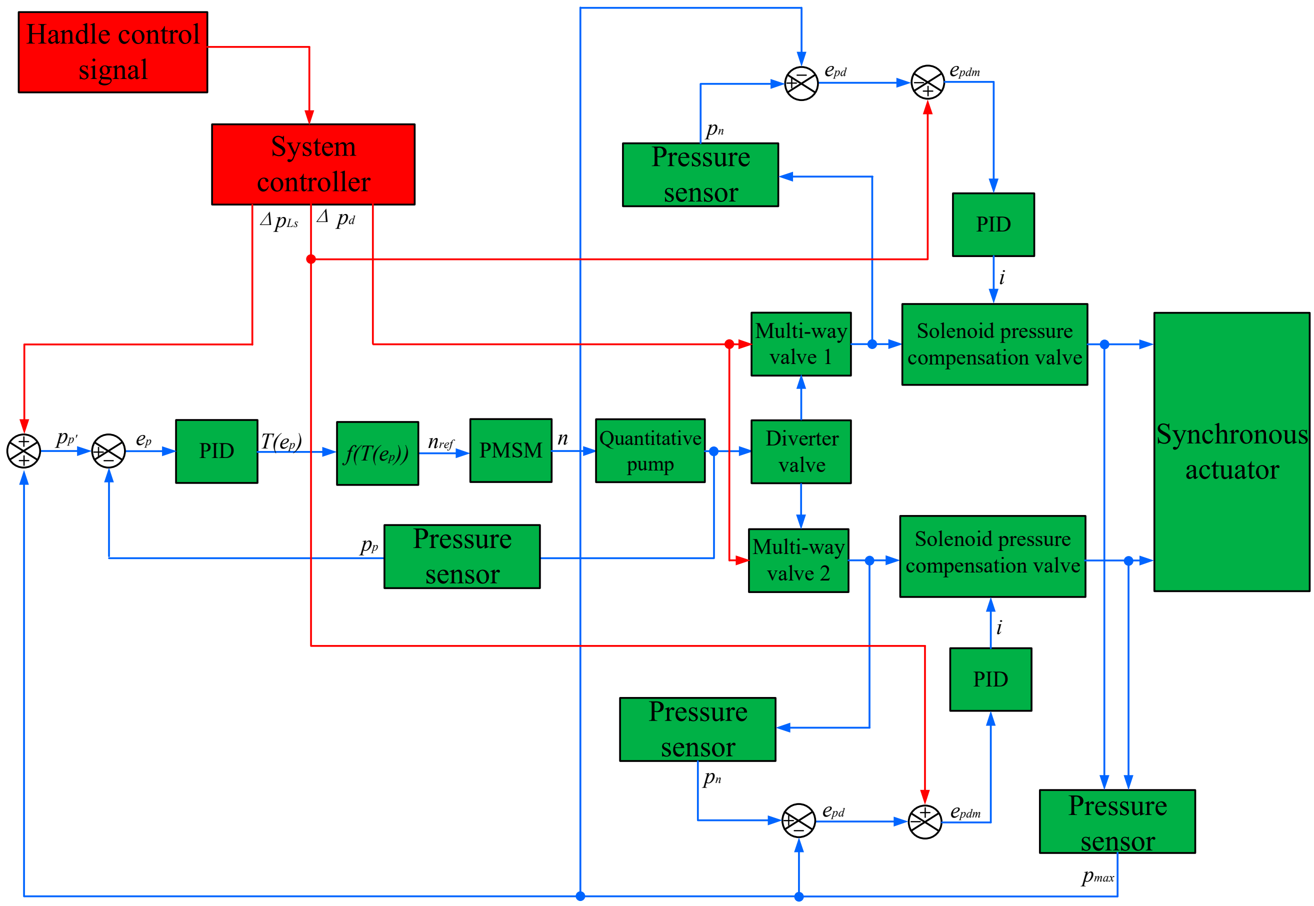

Figure 3. Block diagram of the system control strategy.

4. Analysis of Components' Mathematical Model

This part analyzes the PMSM, solenoid pressure compensation valve, and diverter valve mathematical model and establishes the components simulation model based on the mathematical model.

4.1. PMSM Mathematical Model

The PMSM consists of a controller, inverter, motor, and sensors. In order to facilitate the analysis, the assumptions are simplified during the derivation of the mathematical model [25]. Based on the assumptions, its equivalent schematic diagram can be obtained, as shown in Figure 4.

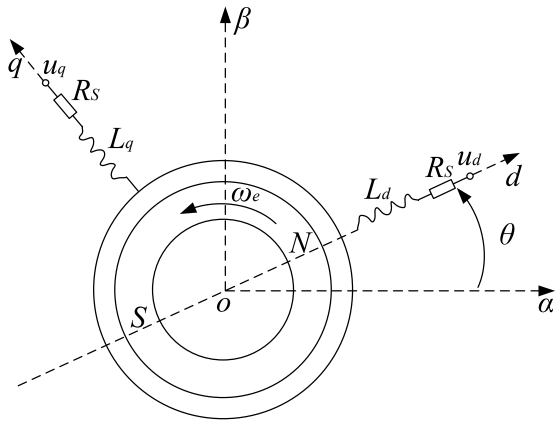

Figure 4. Equivalent schematic of the PMSM in dq coordinate system.

The stator voltage equation of the PMSM can be described as [25]:

$$\begin{bmatrix} u_d \\ u_q \end{bmatrix} = \begin{bmatrix} R_s & -\omega_e L_q \\ \omega_e L_d & R_s \end{bmatrix} \begin{bmatrix} i_d \\ i_q \end{bmatrix} + \frac{d}{dt} \begin{bmatrix} \psi_d \\ \psi_q \end{bmatrix} + \begin{bmatrix} 0 \\ \omega_e \psi_f \end{bmatrix} \tag{12}$$

where u_d and u_q are the dp-axis voltages, V; i_d and i_q are the dp-axis currents, A; ψ_d and ψ_q are the dp-axis magnetic chains, Wb; and ω_e is the rotor angular velocity, rad/s.

The magnetic chain equation of the PMSM can be described as [25]:

$$\begin{bmatrix} \psi_d \\ \psi_q \end{bmatrix} = \begin{bmatrix} L_d & 0 \\ 0 & L_d \end{bmatrix} \begin{bmatrix} i_d \\ i_q \end{bmatrix} + \begin{bmatrix} \psi_f \\ 0 \end{bmatrix} \tag{13}$$

The electromagnetic torque equation of the PMSM can be described as [25]:

$$T_{2e} = \frac{3}{2} p_{2n} \left[\psi_f i_q + \left(L_d - L_q \right) i_d i_q \right] \tag{14}$$

where T_{2e} is the motor output torque, N·m, and p_{2n} is the number of motor pole pairs.

Equation (14) consists of two terms. The first term, $\psi_f i_q$, is the excitation torque; the electromagnetic torque formed by the interaction of the excitation field of the permanent magnet with the stator current. The second term, $\left(L_d - L_q \right) i_d i_q$, is the reluctance torque; the electromagnetic torque formed by the rotor convex polarity effect. The reluctance torque is inherent to the convex polarity PMSM. There is no formation of reluctance torque for the hidden polarity PMSM due to $L_d \neq L_q$. Therefore, the linear equation of the electromagnetic torque can be described as [25]:

$$T_{2e} = \frac{3}{2} p_n \psi_f i_q \tag{15}$$

The PMSM equations of motion can be described as [25]:

$$T_{3e} = T_L + J \frac{d\omega}{dt} + B\omega \tag{16}$$

where T_{3e} is the motor outlet torque, N·m; T_L is the load torque, N·m; J is the equivalent moment of inertia converted to the motor shaft, kg·m^2; B is the coefficient of viscous friction; and ω is the mechanical angular velocity of the motor outlet shaft, rad/s.

In Equation (16), $B\omega$ is the loss torque of the motor motion and $J\frac{d\omega}{dt}$ is the acceleration torque of the whole motor system. Neglecting the damping efficiency and simplifying Equation (16), we obtain:

$$J \frac{d\omega}{dt} = T_{3e} - T_L \tag{17}$$

The control of the PMSM speed control system can be categorized into variable voltage and frequency, direct torque, speed without a sensor, and vector control [26]. This research uses a representative control method, the $i_{dref} = 0$ control in a vector. Based on the above analysis, the AMESim establishes the simulation model, as shown in Figure 5.

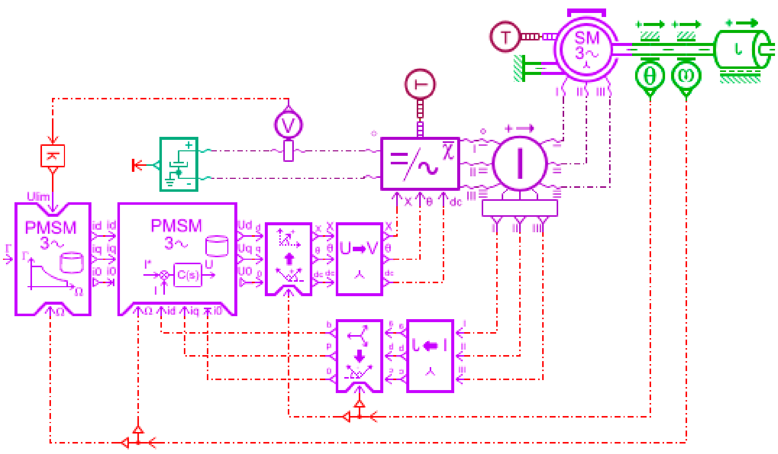

Figure 5. Simulation model of the PMSM.

4.2. Mathematical Modeling of Solenoid Pressure Compensation Valve

The system pressure is controlled by the spool displacement during the operation of the solenoid pressure compensation valve. The differential equation of the spool motion of the pressure compensation valve can be described as follows [27]:

$$F_C - F_K = M_C \frac{d^2 x_C}{dt^2} + B_C \frac{dx_C}{dt} + K_{SC} x_C \tag{18}$$

where F_C is the electromagnetic force, N; F_K is the preset spring force, N; M_C is the spool mass, kg; B_C is the viscous damping coefficient; K_{SC} is the spring stiffness, N/m; and x_C is the spool displacement, m.

For the maximum load branch, the pressure before the solenoid pressure compensation valve can be described as [27]:

$$p_{C1} = \Delta p_d + p_{max} \tag{19}$$

where p_{C1} is the pressure before the solenoid pressure compensation valve, Pa.

For the other branch, the pressure before the solenoid pressure compensation valve can be described as [27]:

$$p_{C2} = \Delta p_d + p_L + p_C \tag{20}$$

where p_{C2} is the pressure before the solenoid pressure compensation valve, Pa; p_L is the load pressure, Pa; and p_C is the solenoid pressure compensation valve compensating pressure, Pa.

When the load pressure p_{max} and p_L change dynamically, F_C changes with them. It can be seen in Equations (18)–(20) that due to the compensating effect of the solenoid pressure compensation valve, i.e., p_C is compensated in the less loaded branch, making $p_{C1} = p_{C2}$. It makes the pressure difference before and after the multi-way valves, 1 and 2, equal, making the flow rate through the multi-way valves, 1 and 2, equal.

Based on the above analysis, the AMESim hydraulic, signal, and HCD library are used to establish the simulation model, as shown in Figure 6, and the simulation parameters in Table 1.

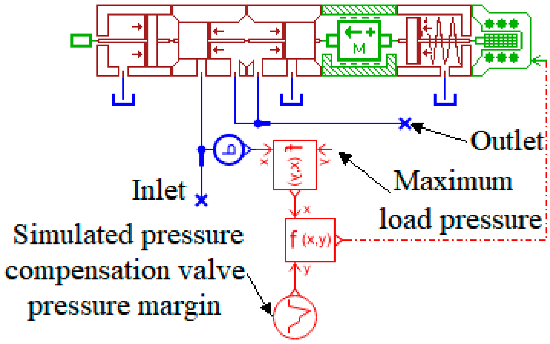

Figure 6. Simulation model of the solenoid pressure compensation valve.

Table 1. The Main simulation parameters of the solenoid pressure compensation valve.

Components	Parameters	Value
Solenoid pressure compensation valve	Spool diameter	0.01 m
	Zero displacement length	0.003 m
	Rated current	0.04 A
	Damping factor	50 N/(m/s)
	Spool quality	0.01 kg

4.3. Mathematical Modeling of the Diverter Valve

The diverter valve is used as the system flow distribution element, ignoring the secondary influences [28], and its mechanical simplified model is shown in Figure 7, in which the throttle ports are all used as thin-walled small holes.

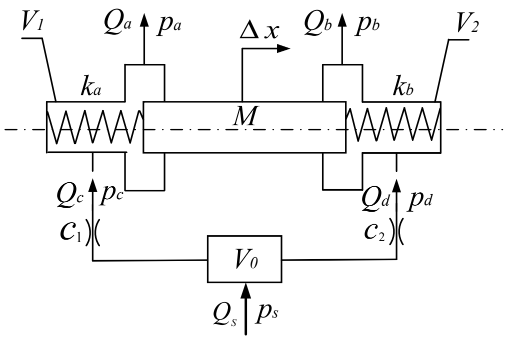

Figure 7. Simplified model of the diverter valve mechanics.

Based on the flow equations for the cylindrical slide valve opening and throttle port, the flow continuity equations for each volume chamber, and the spool dynamics equations, the dynamic mathematical model of the diverter valve can be described as [29]:

$$Q_a = c\pi d_c(x_m + \Delta x)\sqrt{\frac{2}{\rho}(p_c - p_a)} \tag{21}$$

$$Q_b = c\pi d_c(x_m - \Delta x)\sqrt{\frac{2}{\rho}(p_d - p_b)} \tag{22}$$

$$Q_c = \frac{1}{4}c\pi {d_a}^2\sqrt{\frac{2}{\rho}(p_s - p_c)} \tag{23}$$

$$Q_d = \frac{1}{4}c\pi {d_b}^2\sqrt{\frac{2}{\rho}(p_s - p_d)} \tag{24}$$

$$Q_c - Q_a - \frac{1}{4}\pi {d_c}^2\frac{dx}{dt} - \frac{V_1}{\beta_e}\frac{dp_c}{dt} = 0 \tag{25}$$

$$Q_d - Q_b + \frac{1}{4}\pi {d_c}^2\frac{dx}{dt} - \frac{V_2}{\beta_e}\frac{dp_d}{dt} = 0 \tag{26}$$

$$Q_s - Q_c - Q_d - \frac{V_0}{\beta_e}\frac{dp_s}{dt} = 0 \tag{27}$$

$$M\frac{d^2x}{dt^2} + B_v\frac{dx}{dt} + [k_1(x_m + \Delta x) - k_2(x_m - \Delta x)] = \frac{1}{4}\pi {d_c}^2(p_c - p_d) \tag{28}$$

where Q_a and Q_b are the left and right outlet port flow rate, m^3/s; Q_c and Q_d are the outlet flow rate of the left and right cavity fixed throttling ports, m^3/s; Q_s is the inlet port flow rate, m^3/s; c is the throttle port flow coefficient, $c = c_1 = c_2$; d_a and d_b are the equivalent diameters of the fixed throttling holes of the left and right valve cavities, m; d_c is the diameter of the valve seat bore, m; p_a and p_b are the left and right output port pressures, Pa; p_c and p_d are the outlet pressure of the left and right cavity fixed throttling port, Pa; p_s is the inlet port pressure, Pa; x_m is the pre-opening of the variable throttle port when the spool is in the middle position, m; Δx is the pre-opening volume of the convenience throttle port when the spool is in the neutral position, m; V_0 is the inlet cavity volume, m^3; V_1 and V_2 are the left and right cavity volumes of the spool, m^3; β_e is the integrated modulus of elasticity of the system; B_v is the viscous damping of the liquid; M is the mass of the spool, kg; and k_1 and k_2 are the centering spring stiffnesses.

The steady-state characteristic equation of the diverter valve can be obtained by making $\frac{dp_c}{dt} = \frac{dp_d}{dt} = \frac{dp_s}{dt} = \frac{d^2x}{dt^2} = \frac{dx}{dt} = 0$.

The system diverter error can be described as:

$$\eta = 2\frac{Q_a - Q_b}{Q_s} \times 100\% \tag{29}$$

where η is the system diverter error, %.

Based on the above analysis, the AMESim hydraulic, 2D mechanical, and HCD libraries are used to establish the simulation model, as shown in Figure 8, and the simulation parameters in Table 2.

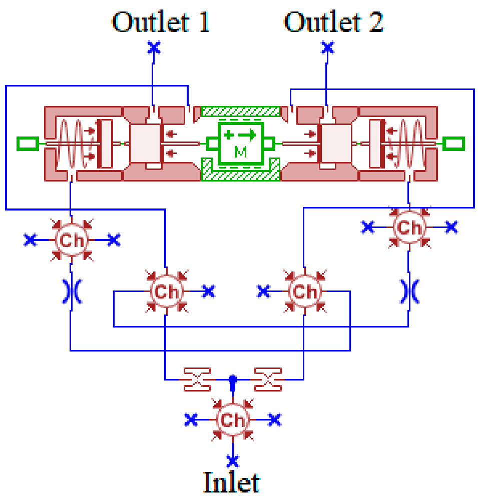

Figure 8. Simulation model of the diverter valve.

Table 2. The main simulation parameters of the diverter valve.

Components	Parameters	Value
Diverter valve	Spring stiffness	1000 N/m
	Spring pre-compression force	10 N
	Spool diameter	0.01 m
	Zero displacement length	0.003 m
	Maximum opening displacement length	0.01 m
	Spool quality	0.01 kg

5. System Modeling and Simulation

This part establishes the simulation models of the EHLS, EHLS synchronous, and EHLS diverter synchronous drive systems and analyzes the system characteristics.

5.1. The EHLS Drive System

Based on the analysis in Section 3.1, Section 3.2, and Section 4.1, the simulation model can be established using the AMESim hydraulic, 1D mechanical, and signal libraries, as shown in Figure 9. The proportional relief valve simulates the load, which is set to $(5\sin(2\pi t) + 20)$ MPa. The proportional throttle valve simulates the multi-way valve. The main simulation parameters of the system are set, as shown in Table 3. The simulation time is set to 10 s, in which 0 to 2 s multi-way valve opening is 20%, 2 s to 4 s multi-way valve opening is 40%, 4 s to 6 s multi-way valve opening is 60%, 6 s to 8 s multi-way valve opening is 80%, and 8 s to 10 s multi-way valve opening is 100%. Subsequent studies will analyze the system characteristics based on this simulation time. The system characteristics are discussed for simulated load-sensitive pressure margins of 2 MPa and 3 MPa, respectively.

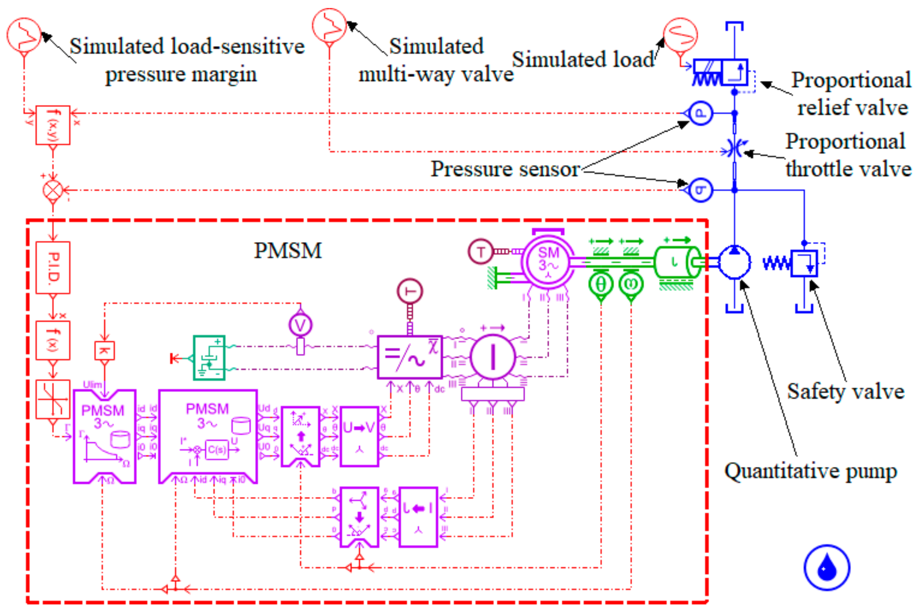

Figure 9. The simulation model of the EHLS drive system.

Table 3. The main simulation parameters of the system.

Components	Parameters	Value
PMSM	Rated speed	1500 rev/min
Quantitative pump	Displacement	0.0002 m^3/rev
	Rated speed	1500 rev/min
Safety valve	Cracking pressure	28 MPa
Proportional throttle	Maximum opening diameter	0.01 m
	Minimum signal	0
	Maximum signal	1
Proportional relief valve	Maximum opening pressure	25 MPa
	Valve lagging pressure	0
	Valve rated current	0.25 A

As shown in Figure 10, the system pressure, flow, and opening curves are simulated when the load-sensitive pressure margin is 2 MPa. The outlet pressure of the quantitative pump changes, and the pressure difference before and after the multi-way valve is maintained at 2 MPa when the simulated load pressure changes. The flow rate through the multi-way valve increases when the opening of the multi-way valve increases. The system flow rate is independent of the load pressure and proportional to the opening of the multi-way valve. Therefore, the system realizes the primary function of the load-sensitive system.

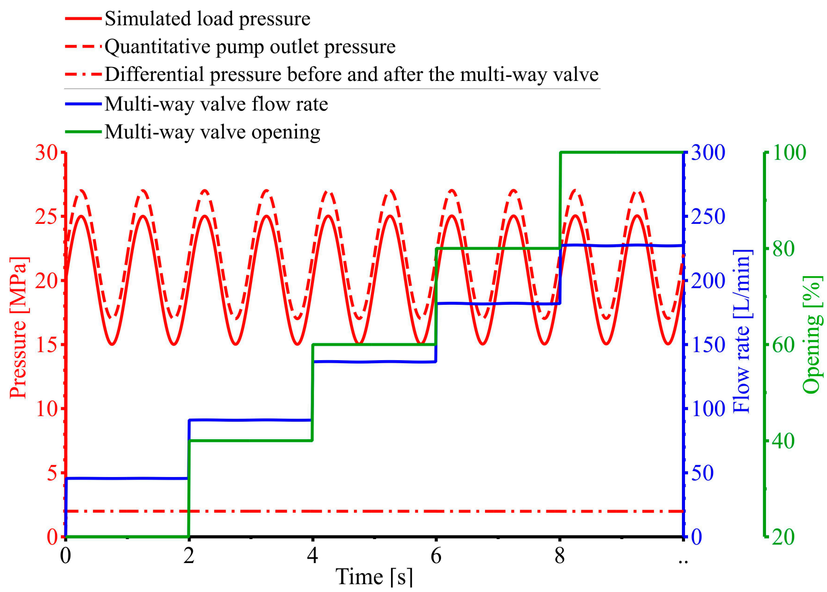

Figure 10. System pressure, flow, and opening curves for the load-sensitive margin of 2 MPa.

As shown in Figure 11, the system pressure, flow, and opening curves are simulated when the load-sensitive pressure margin is 3 MPa. The quantitative pump outlet pressure changes, and the pressure difference before and after the multi-way valve is maintained at 3 MPa when the simulated load pressure changes. The flow rate through the multi-way valve increases when the multi-way valve opening increases. As the simulated load-sensitive pressure margin increases, the flow rate through the multi-way valve increases, combined with the analysis in Figure 10. Therefore, the system can realize variable load-sensitive pressure margin control to regulate the differential pressure and flow rate before and after the multi-way valve.

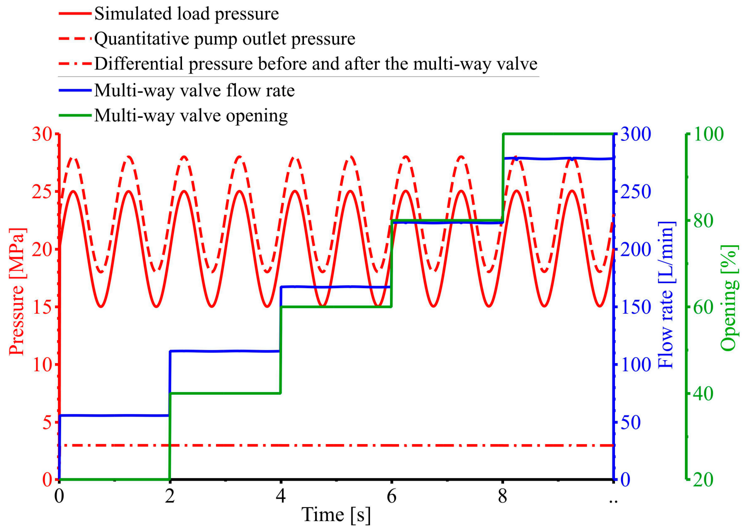

Figure 11. System pressure, flow, and opening curves for the load-sensitive margin of 3 MPa.

Based on the above analysis, the system realizes the primary functions of the load-sensitive system and can realize the variable load-sensitive pressure margin control to regulate the differential pressure and flow before and after the multi-way valve.

5.2. The EHLS Synchronous Drive System

Based on the analysis in Section 3.2 and combined with the analysis in Section 5.1, a simulation model can be established, as shown in Figure 12. The system consists of two synchronous branches: load 1 is set to $(5\sin(4\pi t) + 15)$ MPa and load 2 is set to $(5\cos(4\pi t) + 15)$ MPa. The subsequent study will analyze the system characteristics based on this load. The system characteristics are discussed for simulated solenoid pressure compensation valves with 1 MPa and 1.5 MPa pressure margins, respectively.

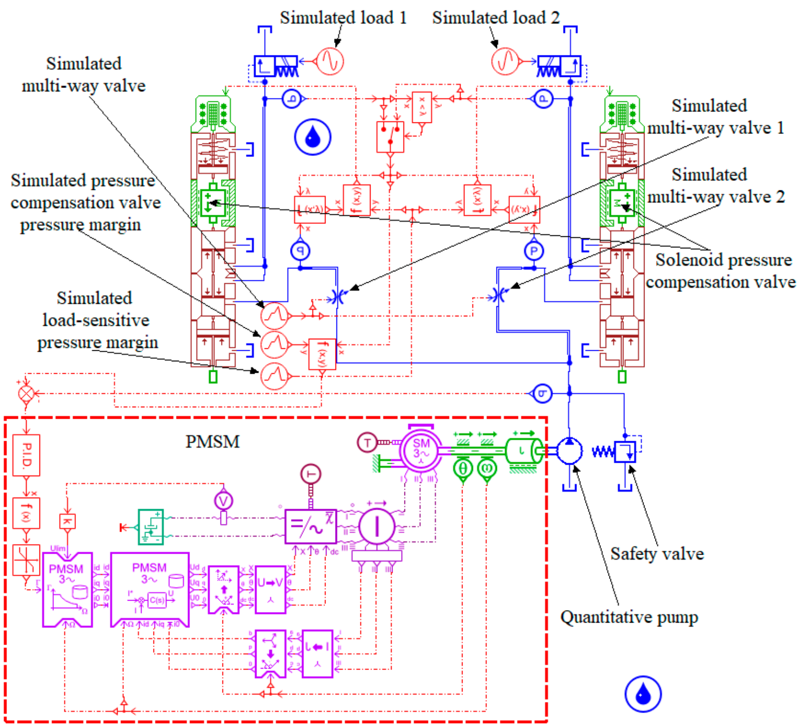

Figure 12. The simulation model of the EHLS synchronous drive system.

As shown in Figure 13, the system pressure, flow rate, and opening curves are shown when the solenoid pressure compensation valve margin is 1 MPa. The pressure difference before and after the multi-way valves, 1 and 2, is maintained at about 1 MPa when the simulated load pressures, 1 and 2, change alternately. The flow rate of the multi-way valves, 1 and 2, gradually increases, and the flow rate error becomes larger and larger as the opening of the multi-way valve increases. Therefore, the system has poor synchronous control accuracy.

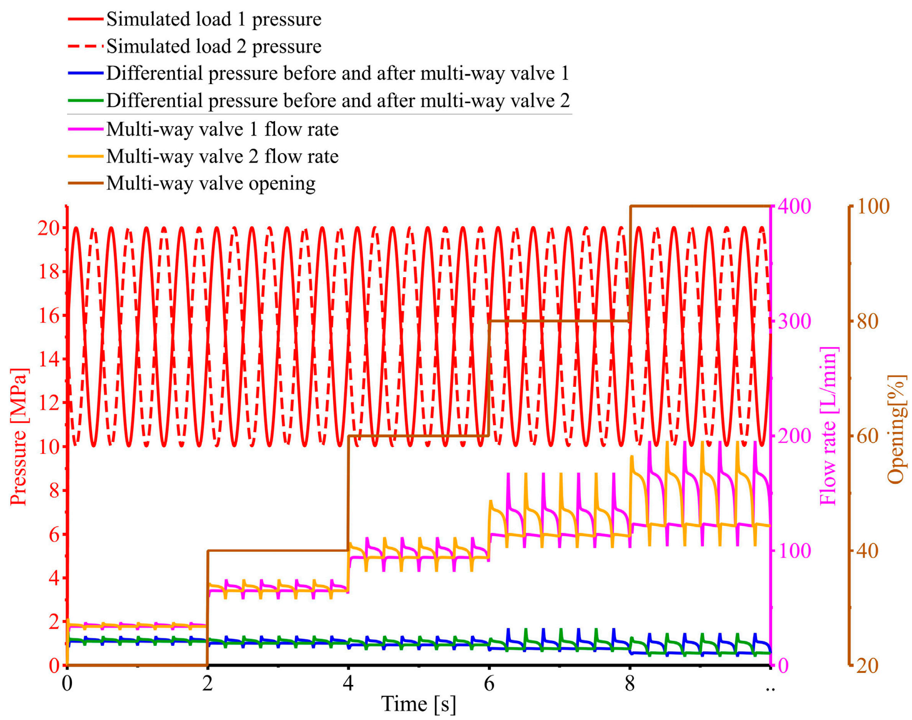

Figure 13. System pressure, flow rate, and opening curves for the solenoid pressure compensation valve of 1 Mpa.

As shown in Figure 14, the system pressure, flow rate, and opening curves are shown when the solenoid pressure compensation valve margin is 1.5 MPa. The pressure difference between the front and rear of the multiplex valves, 1 and 2, is maintained at about 0.5 MPa when the simulated load pressures, 1 and 2, change alternately. The flow rate of the multi-way valves, 1 and 2, gradually increases, and the flow rate error becomes larger and larger as the opening of the multi-way valve increases. As the solenoid pressure compensation valve margin increases, the flow rate through the multi-way valve decreases, combined with the analysis in Figure 13. The differential pressure error before and after the multi-way valves, 1 and 2, is getting smaller and smaller, and the system flow error is getting smaller and smaller. Therefore, the system can realize variable pressure compensation valve pressure margin control to regulate the differential pressure and flow before and after the multi-way valve.

Based on the above analysis, the system has poor synchronous control accuracy. It can realize variable solenoid pressure compensation valve pressure margin control to regulate the pressure difference and flow rate before and after the multi-way valve.

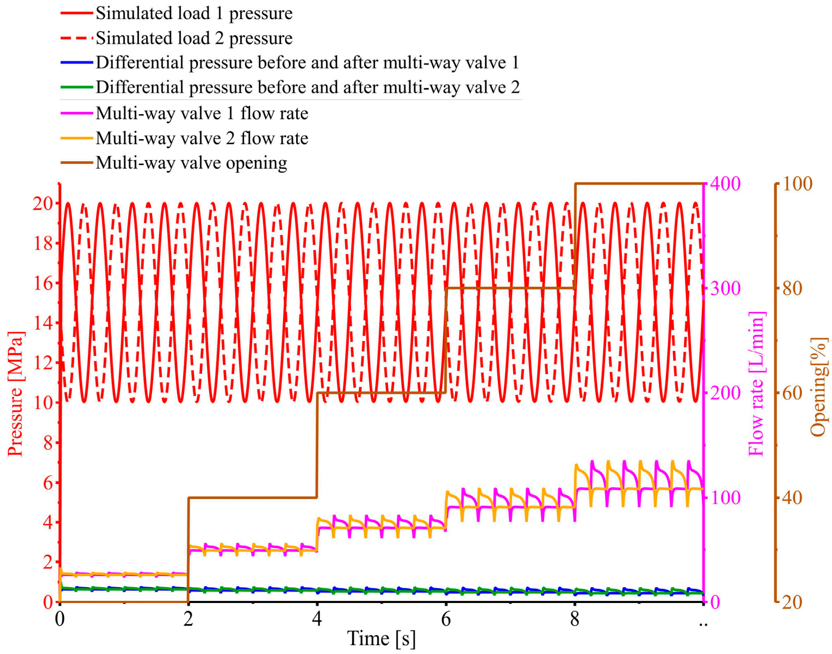

Figure 14. System pressure, flow, and opening curves for the pressure solenoid compensation valve margin of 1.5 MPa.

5.3. The EHLS Diverter Synchronous Drive System

Based on the analysis in Section 3 and combined with the analysis in Section 5.2, the simulation model can be established, as shown in Figures 15 and 16. The diverter valve is added to the EHLS synchronous drive system to construct an EHLS diverter synchronous drive system. The system characteristics are analyzed before and after the variable pressure margin control.

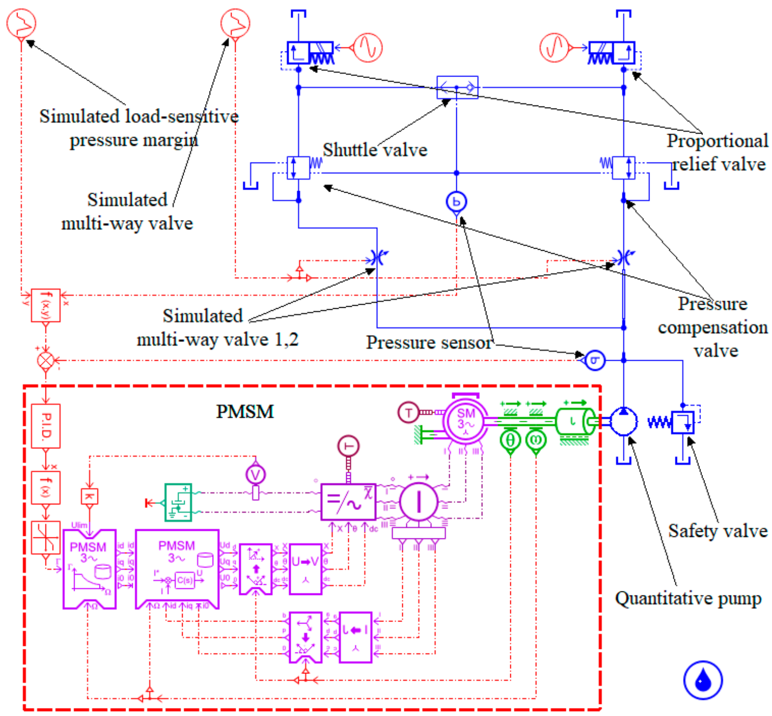

Figure 15. The simulation model of the conventional EHLS diverter synchronous drive system.

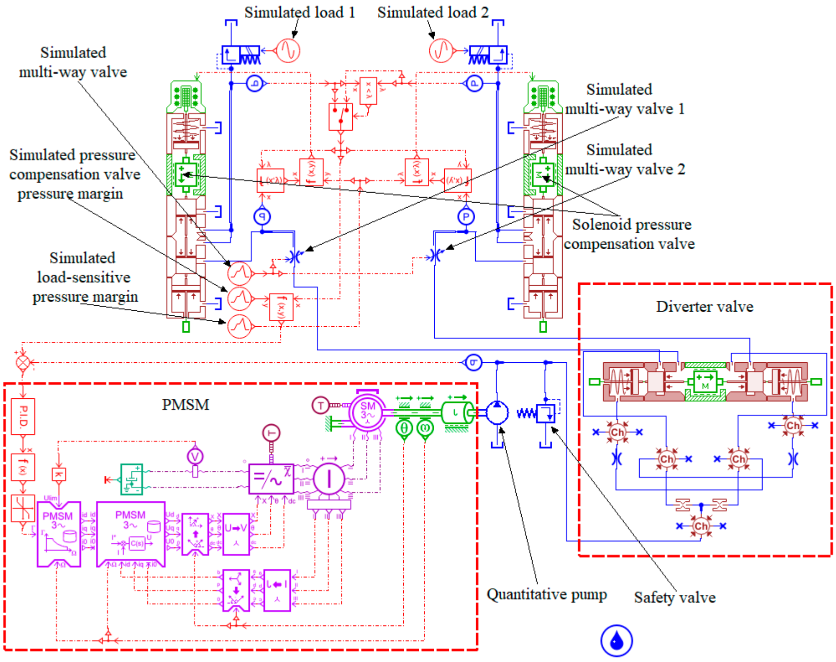

Figure 16. The simulation mode of the EHLS diverter synchronous drive system.

As shown in Figure 17, the system pressure, flow, and opening curves before the variable pressure margin are shown. In the diverter system, as the opening of the multi-way valves increases, the flow rate through the multi-way valve increases. The throttling effect of the diverter valve is enhanced, resulting in a decrease in the pressure difference between before and after the multi-way valves, 1 and 2, compared to the synchronous system, which leads to a decrease in the flow rate through the multi-way valves, 1 and 2. As a result, the synchronous control performance of the system decreases. The differential pressure and flow rate before and after the multi-way valve can be adjusted by variable pressure margin control to improve the synchronous control performance of the system combined with the analysis in Sections 5.1 and 5.2.

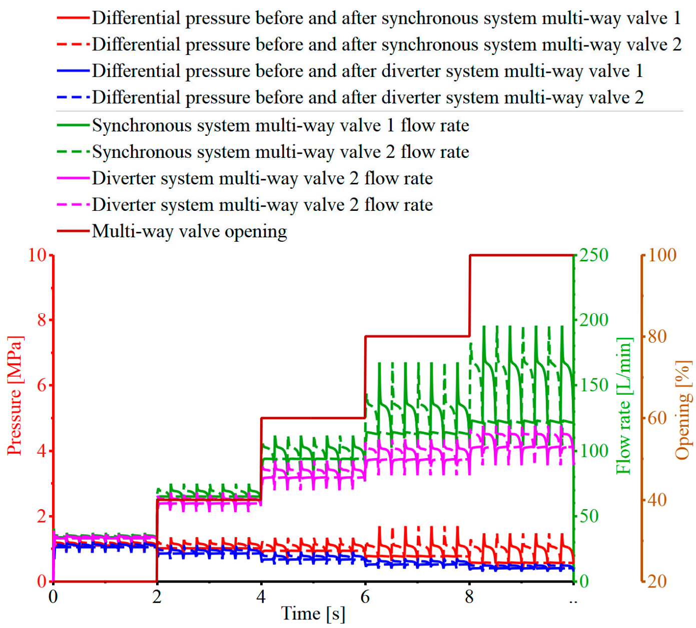

Figure 17. The system pressure, flow, and opening curves before the variable pressure margin.

As shown in Figure 18, the system pressure and opening curves after the variable pressure margin are shown. In the diverter system, after the variable pressure margin control, compared with the before compensation period, the pressure difference before and after the multi-way valve, 1 and 2, increases significantly as the opening of the multi-way valve increases, and it is consistent with the synchronous system, which maintains the pressure difference at about 1 MPa.

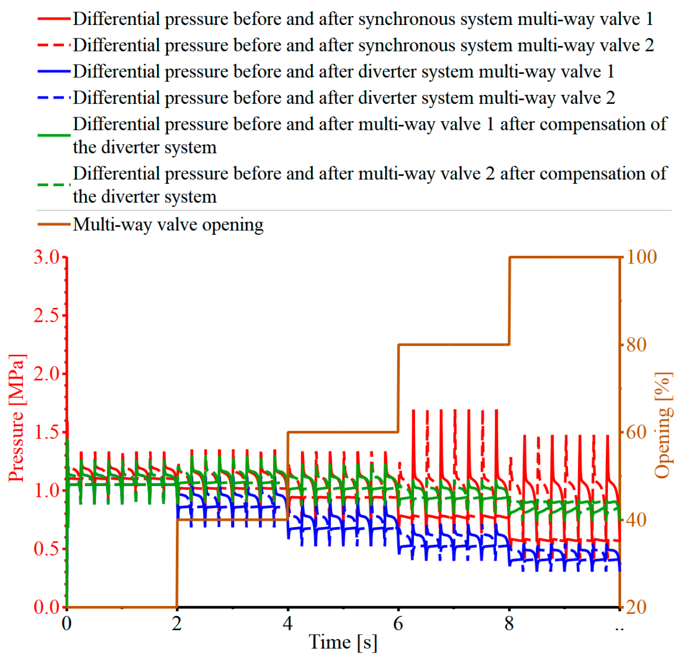

Figure 18. The system pressure and opening curves after the variable pressure margin.

As shown in Figure 19, the system flow and opening curves after the variable pressure margin are shown. In the diverter system, after the variable pressure margin control, compared with the before compensation period, the flow rate of the multi-way valve, 1 and 2, increases significantly as the opening of the multi-way valve increases and is consistent with the synchronous system. Therefore, the diverter system effectively improves the synchronous control performance of the system after compensation by variable pressure margin.

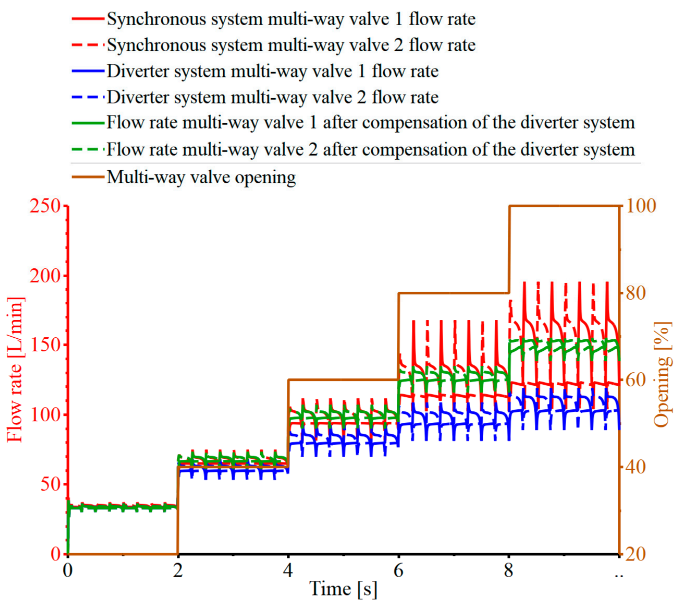

Figure 19. The system flow and opening curves after the variable pressure margin.

As shown in Figure 20, the system diverter error and opening curves are shown. The diverter error of the conventional, the diverter, and the diverter compensation systems gradually increases as the opening of the multi-way valve increases. In particular, the maximum diverter error of the conventional system is 61%, the diverter system is 20.2%, and the diverter system after compensation is 8.4% when the diverter valve is fully opening. Therefore, the diverter system diverter error is reduced by 40.8%, and the diverter system after compensation diverter error is reduced by 52.6%. The diverter system after compensation effectively improves the synchronous accuracy of the system by variable pressure margin compensation control.

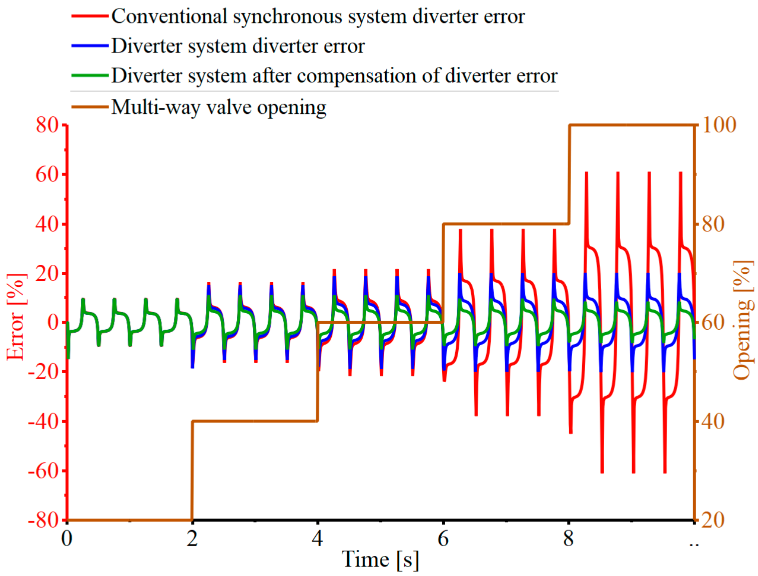

Figure 20. System diverter error and opening curves.

Based on the above analysis, the diverter system effectively improves the synchronous control performance of the system by variable pressure margin compensation control. The diverter system diverter error is reduced by 40.8%, and the diverter error of the diverter system after compensation is reduced by 52.6% when the multi-way valve is fully opening. The diverter system after compensation effectively improves the synchronous accuracy of the system by the variable pressure margin compensation control. In summary, the system performance can be compared, as shown in Table 4.

Table 4. The comparison of the system performance.

Components		System Performance
The EHLS drive system		The variable load-sensitive pressure margin control is realized
The EHLS synchronous drive system		The variable pressure compensation valve pressure margin control is realized
The EHLS diverter synchronous drive system	Conventional system	The system diverter synchronous accuracy is low, and the maximum diverter error is 61%
	Diverter system	The synchronous control performance decreases, the maximum diverter error is 20.2%, and the diverter error is reduced by 40.8%
	Diverter system after compensation	The synchronous control performance is guaranteed, the maximum diverter error is 8.4%, and the diverter error is reduced by 52.6%

6. Discussion

The system working principle, control strategy, and component mathematical model are analyzed. Based on this partial analysis, the EHLS, EHLS synchronous, and EHLS diverter synchronous drive system simulation models were established, respectively, and the system characteristics were analyzed. The simulation results show that the EHLS diverter synchronous drive system effectively improves the diverter synchronous accuracy of the system. It guarantees the system's synchronous control performance compared with the conventional EHLS synchronous drive system through the variable pressure margin compensation control.

This EHLS diverter synchronous drive system and diverter valve combine an EHLS synchronous drive system. They effectively improve the diverter synchronous accuracy of the system through the diverter valve diverter effect and variable pressure margin control. The system is suitable for the actuator action, the system of each branch of the time-varying load, and the actuator synchronous accuracy requirements of high occasions. The variable pressure margin control system can ensure that the system still has a high diverter synchronous accuracy when the multi-way valve has different opening degrees.

7. Conclusions

Based on the above, the following conclusions can be obtained:

1. The EHLS drive system realizes the primary function of the load-sensitive system. It can realize the variable load-sensitive pressure margin control to regulate the differential pressure and flow rate before and after the multi-way valve;
2. The EHLS synchronous drive system has poor synchronous control accuracy. It can realize variable pressure compensation valve pressure margin control to regulate the differential pressure and flow before and after the multi-way valve;
3. The EHLS diverter synchronous drive system effectively improves the synchronous control performance of the system through variable pressure margin compensation control. The diverter system diverter error is reduced by 40.8%, and the diverter compensation system diverter error is reduced by 52.6% when the multi-way valve is fully opened. After the variable pressure margin compensation control, the diverter system effectively improves the diverter synchronous accuracy;
4. The system provides a high-performance hydraulic synchronous drive solution under severe working conditions.

Author Contributions: Conceptualization and methodology, W.D.; software, validation, and writing—original draft preparation, W.D., H.M. and Y.L. (Yu Luo); writing—review and editing and supervision, project administration, and funding acquisition, Y.L. (Yu Luo) and Y.L. (Yanlei Luo). All authors have read and agreed to the published version of the manuscript.

Funding: This work is supported by the National Natural Science Foundation of China Project (52265007) and the Science and Technology Project of Guizhou Province (Qiankehe Foundation-ZK (2022) General 087).

Data Availability Statement: Data are contained within the article.

Acknowledgments: We would like to express our gratitude to the anonymous reviewers and friends who helped us in the process of completing this paper.

Conflicts of Interest: The authors declare no conflict of interest.

References

1. Wang, H. Analysis of Current Situation and Prospect of Electrification of Construction Machinery. *Constr. Mach. Dig.* **2022**, *3*, 23–25.
2. Nie, H.; Shen, W. Research on Popularization and Application of Electric Construction Machinery. *Constr. Mech.* **2022**, *43*, 19–21.
3. Fu, S.; Lin, T.; Wang, L.; Miao, C. Load Sensitive System Based on Variable Speed Control. *China J. Highw. Transp.* **2020**, *33*, 189–196.

4. Zuo, D.; Qian, L.; Yang, T.; Cui, X.; Luo, Q. Coupling Leveling Control Based on Fuzzy PID for Synchronous Loading System of Load-Bearing Test Bed. *Chin. J. Electron.* **2017**, *26*, 1206–1212. [CrossRef]
5. He, B.; Zhao, C.; Wang, H.; Chang, X.; Wen, B. Dynamics of synchronization for four hydraulic motors in a vibrating pile driver system. *Adv. Mech. Eng.* **2016**, *8*, 1–15. [CrossRef]
6. Liu, Z.; Gao, Q.; Yu, C.; Li, X.Y.; Guan, W.L.; Deng, G.F. Collaborative Synchronization Digital Control for Double Hydraulic Cylinders. *Adv. Mech. Eng.* **2014**, *6 Pt 9*, 371403. [CrossRef]
7. Wang, X.; Liao, R.; Shi, C.; Wang, S. Linear extended state observer-based motion synchronization control for hybrid actuation system of more electric aircraft. *Sensors* **2017**, *17*, 2444. [CrossRef] [PubMed]
8. Rehman, U.; Wang, X.; Hameed, Z.; Gul, M.Y. Motion Synchronization Control for a Large Civil Aircraft's Hybrid Actuation System Using Fuzzy Logic-Based Control Techniques. *Mathematics* **2023**, *11*, 1576. [CrossRef]
9. Ding, H.; Liu, Y.; Zhao, J.; Chao, C. Research on principle of variable speed flow dividing synchronous drive in load-sensing under time-varying bias loads. *J. Huazhong Univ. Sci. Technol. (Nat. Sci. Ed.)* **2021**, *49*, 62–67.
10. Ding, H.; Liu, Y.; Zhao, Y. A new hydraulic synchronous scheme in open-loop control: Load-sensing synchronous control. *Meas. Control* **2020**, *53*, 119–125. [CrossRef]
11. Li, R.; Yuan, W.; Ding, X.; Xu, J.; Sun, Q.; Zhang, Y. Review of Research and Development of Hydraulic Synchronous Control System. *Processes* **2023**, *11*, 981. [CrossRef]
12. Ma, T.; Guo, X.; Su, G.; Deng, H.; Yang, T. Research on Synchronous Control of Active Disturbance Rejection Position of Multiple Hydraulic Cylinders of Digging-Anchor-Support Robot. *Sensors* **2023**, *23*, 4092. [CrossRef] [PubMed]
13. Ding, H.; Wang, Y.; Zhang, H. Robust Output Feedback Position Control of Hydraulic Support with Neural Network Compensator. *Actuators* **2023**, *12*, 263. [CrossRef]
14. Guo, Y.; Zhang, Z.; Liu, Q.; Nie, Z.; Gong, D.W. Decoupling-based adaptive sliding-mode synchro-position control for a dual-cylinder driven hydraulic support with different pipelines. *ISA Trans.* **2021**, *123*, 357–371. [CrossRef] [PubMed]
15. Zhu, C.; Zhang, H.; Wang, W.; Li, K.; Zhou, Z.; He, H. Compound Control on Constant Synchronous Output of Double Pump-Double Valve-Controlled Motor System. *Processes* **2022**, *10*, 528. [CrossRef]
16. Yao, J.; Cao, X.; Zhang, Y.; Li, Y. Cross-coupled fuzzy PID control combined with full decoupling compensation method for double cylinder servo control system. *J. Mech. Sci. Technol.* **2018**, *32*, 2261–2271. [CrossRef]
17. Mu, H.; Luo, Y.; Deng, H.; Du, W.; Liu, Y. Simulation study on load-sensing shunt synchronous drive of agricultural machinery. *Mach. Tool Hydraul.* **2022**, *50*, 164–168.
18. Hu, J.; Wang, X.; Liu, C. Research on design of load sensitive synchronous control hydraulic system of static pile driver. *Manuf. Autom.* **2021**, *43*, 94–98.
19. Yang, L.; Yang, C.; Zhang, Y.; Wang, Q. Design of Load Sensitive Synchronous Drive System and Analysis of Synchronous Characteristics. *Constr. Mach. Equip.* **2021**, *52*, 97–102+12.
20. Wang, F.; Zhao, J.; Liu, J.; Li, H. Simulation Research of Synchronous System with Large Eccentric Loads Based on Load-Sensing Principle. *Mach. Tool Hydraul.* **2017**, *45*, 142–144.
21. Yang, X. Research on the Hydraulic Synchronous Control System in Load-Sensing NC Bending Machine. Master's Thesis, Anhui University of Technology, Maanshan, China, 2016.
22. Ding, H.; Liu, Y.; Zhao, J. Load Sensitive Variable Speed Synchronous Drive Principle and Characteristics. *Chin. Hydraul. Pneum.* **2021**, *45*, 77–81.
23. Cheng, M.; Yu, J.; Ding, R. Electrohydraulic Load Sensing System via Compound Control of Flow Feedforward and Pressure Feedback. *J. Mech. Eng.* **2018**, *54*, 262–270. [CrossRef]
24. Du, L. Research on Load-Sensitive System of Hydrostatic Drive Rotary Tiller. Master's Thesis, Guizhou University, Guiyang, China, 2022.
25. Yu, X. Research on Dual-Variable Control Algorithm of Electro-Hydrostatic Actuator. Master's Thesis, Beijing Jiaotong University, Beijing, China, 2020.
26. Qin, D. Research and Implementation of PMSM-DTC System. Master's Thesis, Anhui University of Science and Technology, Huainan, China, 2018.
27. Chen, W. Research on Hybrid Pressure Compensation Hydraulic Control System. Master's Thesis, Guizhou University, Guiyang, China, 2021.
28. Liu, Y. Study on Load Sensitive Variable Speed Flow Dividing Principle and Synchronous Drive Characteristics. Master's Thesis, China University of Mining and Technology, Xuzhou, China, 2021.
29. Chen, L.; Liu, Z.; Zhu, W. Simulation and Research on Dynamic Performance of Hydraulic Diverter Valve. *Constr. Mach. Equip.* **2004**, *9*, 42–45+1.